analytical chemistry

Letter

Cite This: *Anal. Chem.* 2019, 91, 6981−6985

pubs.acs.org/ac

Telomerase Triggered DNA Walker with a Superhairpin Structure for Human Telomerase Activity Sensing

Jing Huang, Longyi Zhu, Huangxian Ju, and Jianping Lei*

State Key Laboratory of Analytical Chemistry for Life Science, School of Chemistry and Chemical Engineering, Nanjing University, Nanjing 210023, P. R. China

Supporting Information

ABSTRACT: Different from conventional DNA walkers, we designed a telomerase-triggered three-dimensional DNA walker consisting of a superhairpin structure with a bulged loop in the stem as the walking strand and dye-labeled tracks for ultrasensitive detection of telomerase activity. In the presence of telomerase, the primers in the stem of the superhairpin structure were elongated and triggered internal strand displacement, thus activating the superhairpin structure. Subsequently, the open superhairpin structure as a swing arm was able to bind with the track, and the swing arm could be released by enzymatic cleavage of the binding duplex domain, resulting in the fluorescence recovery of dye-labeled fragments from the surface of gold nanoparticles. Based on signal amplification of the telomerase-triggered DNA walker, the walking device was further applied to various cancer lines with a low detection limit of telomerase activity equivalent to 90 cells μL^{-1} for HeLa cells. Moreover, the advantage of this DNA walker strategy was confirmed by calculating telomerase activity in a single cell. This telomerase-triggered DNA walker provides a new concept on signal transduction for telomerase detection and is anticipated to stimulate interest in DNA nanomachine design for bioanalysis.

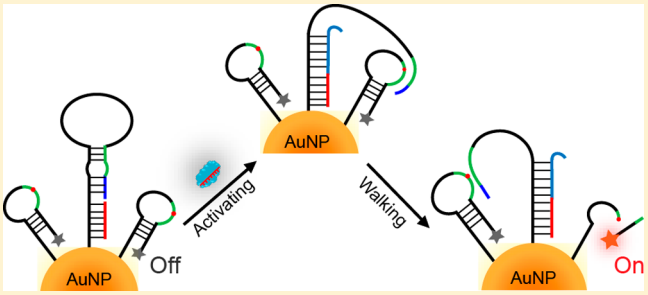

Telomerase is a specialized reverse transcriptase that can maintain genomic stability and cell viability by adding telomeric repeats (5′-TTAGGG-3′) to the 3′ end of telomeres.[1] Due to its high expression in more than 85% of cancer cells,[2,3] telomerase is considered as an important diagnostic and prognostic cancer biomarker.[4] In the past decades, various signal amplification strategies[5,6] have been designed for detection of telomerase activity such as exponential isothermal amplification of telomere repeat,[7] exonuclease-assisted target recycling amplification,[8] DNAzyme-assisted signal amplification,[9] rolling circle amplification,[10] catalyzed hairpin assembly amplification, and so on.[11] To the best of our knowledge, there are few reports on using DNA walker as the signal amplification approach for detection of telomerase activity.[12] Overall, two great challenges could be met as follows: (1) how to integrate the telomerase as the trigger to activate the DNA walker system and (2) specific translation of telomerase activity to signal output.

The DNA walker that mimics biological protein motors is a type of molecular machine that can perform mechanical movement at the micro- or nanoscopic scale by biasing Brownian motion.[13] The autonomous movements of walkers can release multiple signal molecules as a result of cleavage by DNAzymes,[14−16] endonucleases,[17] exonucleases,[18] and endogenous enzymes[19] for signal amplification in designing detection strategies with high sensitivity. Based on the sequence-specific interaction and stimuli-dependent conformation switch, the DNA walker could be triggered by different ways, such as hybridization,[20] pH variation,[21,22] click chemistry reaction,[23] allosteric switch of aptamers,[24] and light,[25,26] demonstrating powerful recognition ability in biosensing. For example, He's group developed a three-dimensional DNA walker driven by the catalyst triggered hairpin catalytic assembly for the detection of DNA.[27] Ye's group engineered a DNA nanomachine activated by target miRNA binding to drive the movement of the walking leg.[28] In terms of protein-responsive biosensors, the common practice is to integrate affinity binding motifs into the DNA walker in order to achieve binding-induced assembly between proteins and affinity ligands for target recognition and signal transduction.[29] In this work, we designed a DNA walker directly triggered by telomerase for detection of enzyme activity.

The DNA walker system was established by assembly of hairpin DNA strands as the tracks and superhairpin components hybridized with telomerase primers (TP) as the swing arm on the single gold nanoparticle (tsDNA-Au) (Scheme 1). Unlike traditional stem-loop hairpins, the swing arm has a five base-pair (bp) bulged loop protruding in the stem to form a superhairpin structure, which separates the stem into two parts, a 10-bp domain for DNA strand displacement and a 5-bp domain (Figure S1). Upon addition

Received: March 31, 2019
Accepted: May 17, 2019
Published: May 17, 2019

DOI: 10.1021/acs.analchem.9b01603
Anal. Chem. 2019, 91, 6981−6985

Scheme 1. Schematic Illustration of Telomerase-Triggered DNA Walker for Detection of Telomerase Activity[a]

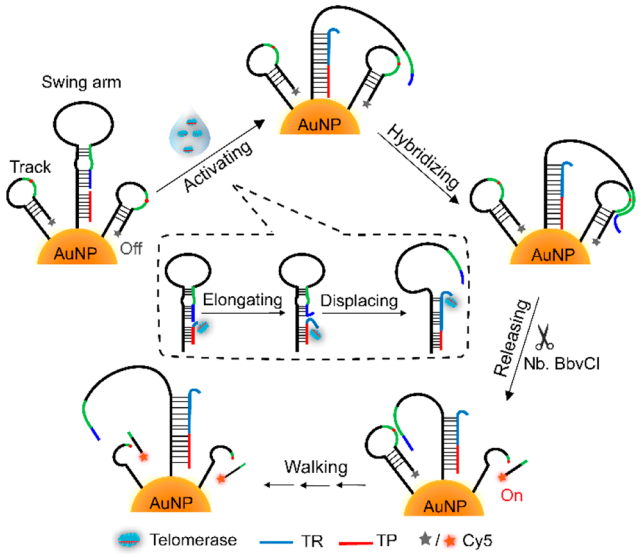

[a]The green domain is the recognition sequence for Nb.BbvCI. The red dot in green domain is the cleavage site.

of telomerase, multiple telomeric repeat units (TR, 5′-TTAGGG-3′) are synthesized from the 3′ end of TP using telomerase's integral RNA as a template. The elongated sequence on the TP region displaces the 10 bp domain in the stem of the swing arm to form more stable double-stranded structures, leading to partial opening of the stem of the swing arm. Sequentially, the remaining 5-bp domain dissociates due to an unstable hairpin conformation at the ambient temperature. Thus, the swing arm is activated and binds with the track to form cleavage site for the endonuclease (Nb.BbvCI). Hydrolysis of the track can release a 14-nt fragment tagged with cyanine 5 (Cy5) from AuNPs and results in the recovery of Cy5 fluorescence. Furthermore, the swing arm is released due to insufficient base pairs with the remaining domain of the hydrolyzed track and subsequently hybridizes to the next track nearby to form a new recognition site. Therefore, autonomous movements of the swing arm could be powered by enzymatic cleavage to release multiple Cy5 tagged oligonucleotides for detection of telomerase activity. The telomerase-triggered DNA walker system provides a new signal transduction platform for evaluating enzyme activity.

The assembly of DNA on AuNPs as the nanocarriers and fluorescent quenchers[30] was adopted via the freezing method[31] rather than the typical salt-aging method.[32] The transmission electron microscopic (TEM) images showed an average diameter of 16 nm for the synthesized AuNPs and good dispersity of tsDNA–Au conjugates after a freeze–thaw cycle (Figure 1A,B), illustrating the successful construction of tsDNA–Au. The dynamic light scattering results indicated that the average hydrodynamic size of AuNPs increased from 24 ± 2 nm to 35 ± 3 nm after DNA assembly (Figure S2). In addition, the characteristic peak of DNA at 260 nm in the UV–vis spectrum of tsDNA–Au indicated the existence of DNA on AuNPs (Figure 1C). Zeta potential analysis showed more negative potential of tsDNA–Au compared to that of AuNPs (Figure 1D), further confirming the successful binding of the DNA onto AuNPs. The density of the track assembled on the gold nanoparticle was evaluated to be around 136 per

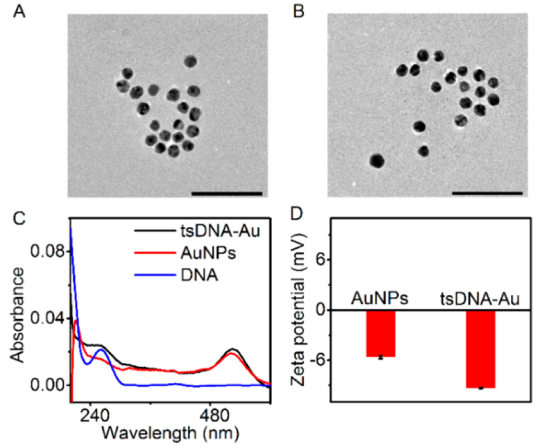

Figure 1. TEM images of (A) AuNPs and (B) tsDNA–Au. Scale bars: 100 nm. (C) UV–vis spectra of AuNPs, DNA, and tsDNA–Au. (D) Zeta potentials (ζ) of AuNPs and tsDNA–Au.

AuNP according to the fluorescent quantitative analysis (Figure S3).

The feasibility of telomerase-triggered TP elongation was verified with polyacrylamide gel electrophoresis (PAGE) in Figure 2A. Comparing with the single band for individual TP

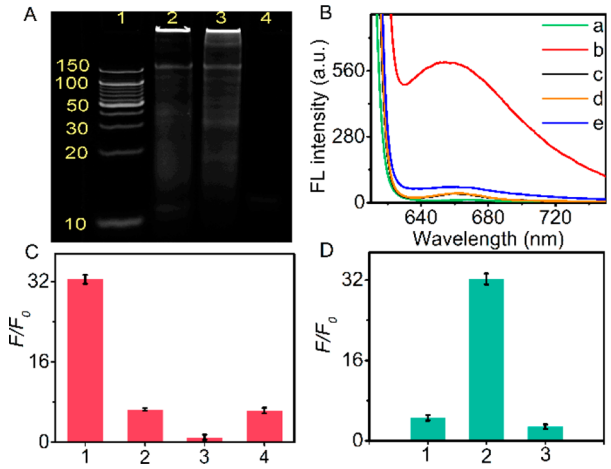

Figure 2. (A) PAGE images of DNA ladder (1), TP (2) and swing arm + TP (3) after incubation with HeLa cell extract at 37 °C for 60 min, and TP (4). (B) Fluorescence emission spectra (λ_{em} = 660 nm) of the designed DNA walker system in the presence of PBS (a), HeLa cell extracts (b), heated HeLa cell extracts (c), CHAPS lysis buffer (d), and the DNA walker system without TP in the presence of HeLa cell extracts (e). (C) Ratio of fluorescence intensity of DNA walker system before (F_0) and after (F) adding telomerase and Nb.BbvCI (1), telomerase (2), Nb.BbvCI (3), and free swing arm + telomerase (4). (D) Dependence of F/F_0 of DNA walker system on the state of swing arm: truncated swing arm (1), swing arm (2), and swing arm in absence of TP (3). F and F_0 are fluorescence intensities of the DNA walker in the presence of cell extracts and heated cell extracts, respectively.

(lane 4), the elongated bands of TP were observed ranging from 30 bp to 150 bp in the presence of cell extracts (lanes 2 and 3), indicating the extension of the TP by telomerase. Moreover, the bands above 150 bp in lane 3 suggested that elongated TP was mostly bound to the swing arm rather than free in solution (Figure S4).

DOI: 10.1021/acs.analchem.9b01603
Anal. Chem. 2019, 91, 6981–6985

To prove the fluorescence response of DNA walker to telomerase, the mixture of tsDNA−Au, dNTPs, and the endonuclease was prepared. The fluorescence intensity of the mixture in PBS showed no obvious fluorescence (Figure 2B, curve a), indicating that DNA walker was inactive and the fluorescence of Cy5 was quenched by AuNPs. Upon addition of HeLa cell extracts, the fluorescence of the mixture was remarkably increased (curve b). Meanwhile, there were very weak fluorescence signals in the addition of CHAPS lysis buffer and heat-treated cell extracts (curves c and d), suggesting that the fluorescence enhancement of the DNA walker resulted from the activated telomerase with high specificity to its corresponding primer (Figure S5). In addition, DNA walker without the telomerase primer showed no fluorescence enhancement with HeLa cell extracts because of no strand displacement occurring (curve e).

To further verify the movement of the walker, walking strands in solution or on the surface of AuNPs were analyzed. Based on the fluorescence increase of track-decorated AuNPs in the presence of the free swing arm for one step, it can be deduced that the swing arm could walk five steps after dividing it into the total fluorescence intensity of the walker system (Figure 2C). Meanwhile, the fluorescence recovery response to telomerase dramatically decreased for the free swing arm compared with swing arms immobilized on the surface of AuNPs. This result suggested that AuNPs could act as three dimension scaffolds to improve hybridization efficiency between tracks and swing arms and accelerate enzymatic cleavage, since the local effective concentration of the track on the AuNP surface is higher than that in the solution.[33] Besides, the length of the swing arm is crucial for walking along multiple tracks and amplifying fluorescence signal for telomerase activity. We prepared a truncated swing arm without the poly-T spacer to verify the effect on movements of the DNA walker. As expected, the fluorescence enhancement plummeted from 32-fold to 4-fold (Figure 2D), indicating that the truncated swing arm could only reach fewer tracks compared with the normal swing arm having a 33-nt T spacer.

To optimize the analytic performance, several parameters of the DNA walker system were investigated. Since there is a competitive effect between tracks and swing arms during assembly on AuNPs resulting in different dynamic ranges of the DNA walker, the concentration ratio between tracks and swing arms was optimized on AuNPs with different sizes (Figures S6 and S7). The DNA walker showed maximal fluorescence enhancement with the molar ratio of the track to swing arm at 20:1, which was chosen as the optimal ratio. The amount of the endonuclease is crucial as the power source for autonomous DNA walking. The value of fluorescence enhancement gradually increases with the increasing of the endonuclease from 0 U to 0.05 U. The amount of the endonuclease is higher than 0.05 U and led to the decrease of fluorescence enhancement (Figure S8A). The reason is that the track could be released by the residue dithiothreitol in a large amount of the endonuclease (Figure S9).[34] Thus, 0.05 U is chosen for the DNA walker system. Different tsDNA−Au concentrations were incubated with cell extracts and the endonuclease, and the fluorescence enhancement of the DNA walker system increased at the beginning and showed the peak value at a concentration of 1.0 nM. The concentration of tsDNA−Au is higher than 1.0 nM and resulted in a slight decrease of the fluorescence enhancement (Figure S8B). Therefore, 1.0 nM was selected as the optimized tsDNA−Au concentration.

As telomerase is broadly expressed in cancer cells, the DNA walker system was applied to detect the activity of telomerase in extracts from HeLa (human cervical cancer cells), MCF-7 (breast cancer cells), and HepG-2 (human liver hepatocellular carcinoma cells) under the optimized conditions. As shown in Figure 3A, the fluorescence of the DNA walker system

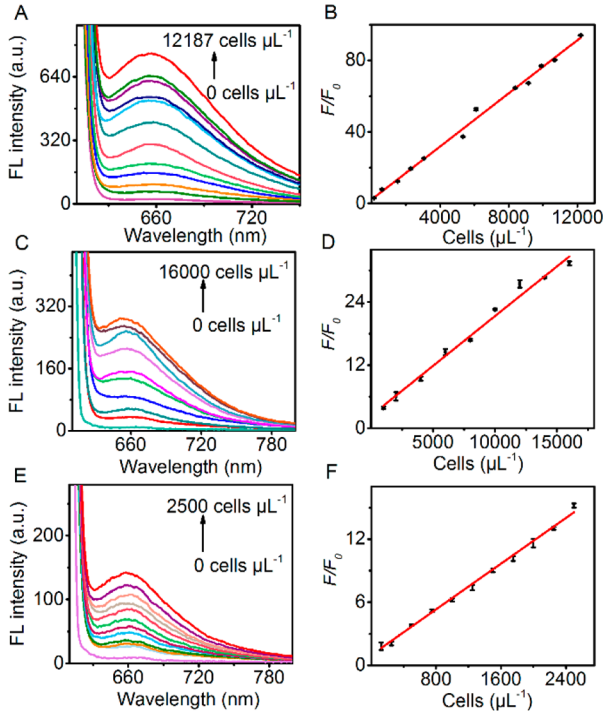

Figure 3. Fluorescence emission spectra of DNA walker incubated with different concentrations of (A) HeLa cell extracts: 0, 152, 609, 1523, 3046, 5331, 6093, 8378, 9140, 9901, 10663, and 12187 cells μL^{-1}. (C) MCF-7 cell extracts: 0, 1000, 2000, 4000, 6000, 8000, 10000, 12000, 14000, and 16000 cells μL^{-1}. (E) HepG2 cell extracts: 0, 125, 250, 500, 750, 1000, 1250, 1500, 1750, 2000, 2250, and 2500 cells μL^{-1}. (B, D, F) Linear relationship between the F/F_0 values and concentrations of cell extracts in parts A, C, and E, respectively ($\lambda_{ex/em}$ = 600/660 nm).

increased with the addition of cell concentration from 0 cells μL^{-1} to 12187 cells μL^{-1}. The fluorescence intensity at 660 nm exhibited a linear correlation with the concentration of HeLa cell extracts (Figure 3B). The linear function is $F/F_0 = 0.0074c + 2.1$ with a correlation coefficient (R^2) of 0.994, where c is the concentration of the HeLa cell extracts. The limit of detection for HeLa cells was calculated to be a telomerase activity equivalent to 90 cells μL^{-1} according to the corresponding telomerase activity. The limits of detection for MCF-7 and HepG-2 cells were calculated to be a telomerase activity equivalent to 316 cells μL^{-1} (R^2 = 0.99) (Figure 3C,D) and 373 cells μL^{-1} (R^2 = 0.996) (Figure 3E,F), respectively. The result showed the remarkable signal-to-noise ratio owing to the finely designed DNA superhairpin structure and inherent specificity of telomerase to its primer. Moreover, the recovery data identified that the fluorescence increase was attributed to telomerase activity but not displacing the substrate of 2-mercaptoethanol in cell extracts (Table S1), suggesting the reliability of our proposed method. Additionally, the relative telomerase activity in the three cell lines was calibrated by

DOI: 10.1021/acs.analchem.9b01603
Anal. Chem. 2019, 91, 6981−6985

enzyme-linked immunosorbent assay using the ELISA standard curve (Figure 4A). As shown in Figure 4B, telomerase activity

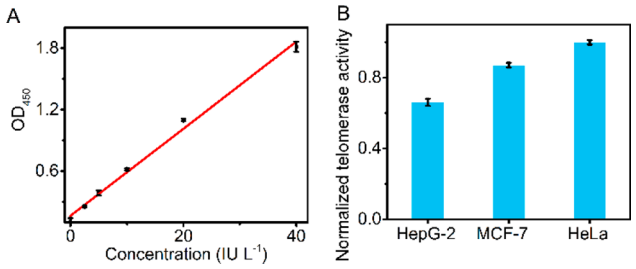

Figure 4. (A) Linear relationship between optical density (OD) at 450 nm and standard telomerase activity using a human telomerase ELISA kit. (B) Normalized telomerase activities in different cell lines evaluated by the DNA walker system.

in each HeLa cell is relatively high (3.72×10^{-9} IU) while relatively low in each MCF-7 cell (3.24×10^{-9} IU) and each HepG-2 cell (2.46×10^{-9} IU), which was in accordance with the previous report.[35] These results indicated that the designed DNA walker could discriminate telomerase activity among different cell lines in biomedical applications.

In summary, by taking advantage of the DNA walker and the biological functions of telomerase, a telomerase-triggered DNA walker is designed for highly sensitive detection of telomerase. The superhairpin structured swing arm hybridized with a telomerase primer not only has the capacity of elongation to initiate DNA strand displacement but also promotes the formation of duplexed recognition sequence between the activated swing arm and the track. The nicking endonuclease hydrolyzes the cleavage site as the power source of DNA walker system to produce multiple Cy5-labeled fragments for signal amplification. The designed DNA walker demonstrates excellent performance to detect telomerase activity with high sensitivity, desirable specificity, and efficiency in cell extracts, providing a new concept on signal transduction for telomerase detection in clinical diagnosis.

■ ASSOCIATED CONTENT

Supporting Information

The Supporting Information is available free of charge on the ACS Publications website at DOI: 10.1021/acs.analchem.9b01603.

Materials and reagents, experimental methods including characterizations, preparation of DNA−AuNP, cell culture, fluorescence spectrum analysis, ELISA, as well as additional spectra and characterization data (PDF)

■ AUTHOR INFORMATION

Corresponding Author

*Phone/fax: +86-25-89681922. E-mail: jpl@nju.edu.cn.

ORCID

Longyi Zhu: 0000-0002-0898-4804
Huangxian Ju: 0000-0002-6741-5302
Jianping Lei: 0000-0002-3594-180X

Notes

The authors declare no competing financial interest.

■ ACKNOWLEDGMENTS

This work was financially supported by the National Natural Science Foundation of China (Grants 21675084, 21605082, and 21890741) and the Natural Science Foundation of Jiangsu Province (Grant BK20160641).

■ REFERENCES

(1) Rudolph, K. L.; Chang, S.; Lee, H. W.; Blasco, M.; Gottlieb, G. J.; Greider, C.; DePinho, R. A. *Cell* **1999**, *96*, 701−712.
(2) Shay, J. W.; Bacchetti, S. *Eur. J. Cancer* **1997**, *33*, 787−791.
(3) Blasco, M. A. *Nat. Rev. Genet.* **2005**, *6*, 611−622.
(4) Harley, C. B. *Nat. Rev. Cancer* **2008**, *8*, 167−179.
(5) Zhou, X. M.; Xing, D. *Chem. Soc. Rev.* **2012**, *41*, 4643−4656.
(6) Xu, L. G.; Zhao, S.; Ma, W.; Wu, X. L.; Li, S.; Kuang, H.; Wang, L. B.; Xu, C. L. *Adv. Funct. Mater.* **2016**, *26*, 1602−1608.
(7) Tian, L. L.; Weizmann, Y. *J. Am. Chem. Soc.* **2013**, *135*, 1661−1664.
(8) Liu, X. J.; Li, W.; Hou, T.; Dong, S. S.; Yu, G. H.; Li, F. *Anal. Chem.* **2015**, *87*, 4030−4036.
(9) Chen, J. B.; Zuehlke, A.; Deng, B.; Peng, H. Y.; Hou, X. D.; Zhang, H. Q. *Anal. Chem.* **2017**, *89*, 12888−12895.
(10) Ma, F.; Wei, S. H.; Leng, J. H.; Tang, B.; Zhang, C. Y. *Chem. Commun.* **2018**, *54*, 2483−2486.
(11) Yan, L. W.; Hui, J. J.; Liu, Y. R.; Guo, Y. H.; Liu, L.; Ding, L.; Ju, H. X. *Biosens. Bioelectron.* **2016**, *86*, 1017−1023.
(12) Xue, J.; Chen, F.; Bai, M.; Cao, X. W.; Huang, P.; Zhao, Y. X. *Anal. Chem.* **2019**, *91*, 4696−4701.
(13) Bath, J.; Turberfield, A. *Nat. Nanotechnol.* **2007**, *2*, 275−284.
(14) Peng, H. Y.; Li, X. F.; Zhang, H. Q.; Le, X. C. *Nat. Commun.* **2017**, *8*, 14378−14390.
(15) Chen, F.; Bai, M.; Cao, K.; Zhao, Y.; Cao, X. W.; Wei, J.; Wu, N.; Li, J.; Wang, L. H.; Fan, C. H.; Zhao, Y. X. *ACS Nano* **2017**, *11*, 11908−11914.
(16) Wang, N. N.; Song, L. R.; Qiu, Y. Q.; Xing, H.; Li, J. S. *Sens. Actuators, B* **2019**, *286*, 250−257.
(17) Wickham, S. F. J.; Bath, J.; Katsuda, Y.; Endo, M.; Hidaka, K.; Sugiyama, H.; Turberfield, A. *Nat. Nanotechnol.* **2012**, *7*, 169−173.
(18) Qu, X. M.; Zhu, D.; Yao, G. B.; Su, S.; Chao, J.; Liu, H. J.; Zuo, X. L.; Wang, L. H.; Shi, J. Y.; Wang, L. H.; Huang, W.; Pei, H.; Fan, C. H. *Angew. Chem., Int. Ed.* **2017**, *56*, 1855−1858.
(19) Chen, F.; Xue, J.; Bai, M.; Qin, J.; Zhao, Y. X. *Chem. Sci.* **2019**, *10*, 3103−3109.
(20) Muscat, R. A.; Bath, J.; Turberfield, A. J. *Nano Lett.* **2011**, *11*, 982−987.
(21) Modi, S.; M. G., S.; Goswami, D.; Gupta, G. D.; Mayor, S.; Krishnan, Y. *Nat. Nanotechnol.* **2009**, *4*, 325−330.
(22) Modi, S.; Nizak, C.; Surana, S.; Halder, S.; Krishnan, Y. *Nat. Nanotechnol.* **2013**, *8*, 459−467.
(23) Qing, M.; Xie, S. B.; Cai, W.; Tang, D. Y.; Tang, Y.; Zhang, J.; Yuan, R. *Anal. Chem.* **2018**, *90*, 11439−11445.
(24) Yan, T. T.; Zhu, L. Y.; Ju, H. X.; Lei, J. P. *Anal. Chem.* **2018**, *90*, 14493−14499.
(25) Yang, Y. Y.; Goetzfried, M. A.; Hidaka, K.; You, M. X.; Tan, W. H.; Sugiyama, H.; Endo, M. *Nano Lett.* **2015**, *15*, 6672−6676.
(26) Yeo, Q. Y.; Loh, I. Y.; Tee, S. R.; Chiang, Y. H.; Cheng, J.; Liu, M. H.; Wang, Z. S. *Nanoscale* **2017**, *9*, 12142−12149.
(27) Li, N. X.; Zheng, J.; Li, C. R.; Wang, X. X.; Ji, X. H.; He, Z. K. *Chem. Commun.* **2017**, *53*, 8486−8488.
(28) Liang, C. P.; Ma, P. Q.; Liu, H.; Guo, X. G.; Yin, B. C.; Ye, B. C. *Angew. Chem., Int. Ed.* **2017**, *56*, 9077−9081.
(29) Zhang, H. Q.; Lai, M. D.; Zuehlke, A.; Peng, H. Y.; Li, X. F.; Le, X. C. *Angew. Chem., Int. Ed.* **2015**, *54*, 14326−14330.
(30) Yun, C. S.; Javier, A.; Jennings, T.; Fisher, M.; Hira, S.; Peterson, S.; Hopkins, B.; Reich, N. O.; Strouse, G. F. *J. Am. Chem. Soc.* **2005**, *127*, 3115−3119.
(31) Liu, B. W.; Liu, J. W. *J. Am. Chem. Soc.* **2017**, *139*, 9471−9474.
(32) Storhoff, J. J.; Elghanian, R.; Mucic, R. C.; Mirkin, C. A.; Letsinger, R. L. *J. Am. Chem. Soc.* **1998**, *120*, 1959−1964.

DOI: 10.1021/acs.analchem.9b01603
Anal. Chem. 2019, 91, 6981−6985

(33) Yang, X. L.; Tang, Y. N.; Mason, S. D.; Chen, J. B.; Li, F. *ACS Nano* **2016**, *10*, 2324−2330.
(34) Li, F.; Lin, Y. W.; Lau, A.; Tang, Y. N.; Chen, J. B.; Le, X. C. *Anal. Chem.* **2018**, *90*, 8651−8657.
(35) Ling, P. H.; Lei, J. P.; Jia, L.; Ju, H. X. *Chem. Commun.* **2016**, *52*, 1226−1229.

DOI: 10.1021/acs.analchem.9b01603
Anal. Chem. 2019, 91, 6981−6985